Let (h_1,h_2,h_3) represent the points in the minimum repeat volume for Q_x below the shaded plane in Fig. 1(*b*). Then (h_1',h_2',h_3') represents the points above the shaded plane; from equation (C.7) it is evident that when Q_x is known in the points (h_1,h_2,h_3) it is also known in the points (h_1',h_2',h_3'). Note that instead of the shaded plane in Fig. 1(*b*) any plane could be chosen containing a line which is parallel to the h_3 axis and goes through the point $(\frac{1}{4},\frac{1}{4},\frac{1}{4})$.

In Appendix I, $Q_x(h_1, h_2, h_3)$, $Q_x(h_2, h_1, h_3)$ and $Q_x(h_3,h_1,h_2)$ were derived, where (h_1,h_2,h_3) represents the points within the basic tetrahedron in Fig. 1(*a*). Due to the symmetries of Q_x (Sparks & Borie, 1966) we have

$$Q_x(-h_2,-h_1,h_3)=-Q_x(h_2,h_1,h_3)\,, \qquad \text{(C.8)}$$

and from the same type of reasoning as above we get

$$Q_x[(\tfrac{1}{2}-h_3),h_2,(\tfrac{1}{2}-h_1)]=-Q_x(h_3,h_2,h_1)\,.$$

The points (h_1,h_2,h_3), $(-h_2,-h_1,h_3)$ and $|(\frac{1}{2}-h_3),h_2,(\frac{1}{2}-h_1)|$ together fill out the part of the minimum repeat volume for Q_x below the shaded plane in Fig. 1 (b). [This can easily be checked by inserting the values for h_1,h_2,h_3 of the basic tetrahedron in Fig. 1(*a*)]. Thus, Q_x is known in its whole minimum repeat volume. The same type of reasoning leads to the conclusion that also R_x and S_{yz} are known in their minimum repeat volumes.

We thank Professor J. E. Gragg, Jr for pointing out to us the additional symmetry for b.c.c. systems that allows this separation.

References

BATTERMAN, B., CHIPMAN, D. R. & DE MARCO, J. (1961). *Phys. Rev.* **122**, 68.

BORIE, B. & SPARKS, C. J. (1971). *Acta Cryst.* In the press.

COOPER, M. J. (1963). *Acta Cryst.* **16**, 1067.

CROMER, D. T. & WABER, J. T. (1965). *Acta Cryst.* **18**, 104.

GEHLEN, P. C. & COHEN, J. B. (1965). *Phys. Rev.* **139**, A844.

GRAGG, J. (1970). PhD thesis. Northwestern Univ., Evanston, Ellinois.

HANSEN, M. (1958). *The Constitution of Binary Alloys.* New York: McGraw-Hill.

HEINRICH, K. F. J. (1966). *The Electron Microprobe.* New York: John Wiley.

HORNBOGEN, E. (1961). *Z. Metallk.* **52**, 47. *J. Appl. Phys.* **32**, 135.

HORNBOGEN, E. (1966). *Arch. Eisenhüttenw.* **37**, 523.

International Tables for X-ray Crystallography. (1962). Vol. III. Birmingham: The Kynoch Press.

KETTUNEN, P. & FORSTÉN, Y. (1964). *Acta Pol. Scand.* ch. 27, 5.

MARCUS, H. L., FINE, M. E. & SCHWARTZ, L. H. (1967). *J. Appl. Phys.* **38**, 4750.

SCHWARTZ, L. H., MORRISON, L. A. & COHEN, J. B. (1963). *Advances in X-ray Analysis.* Vol. 7. New York: Plenum Press.

SINHA, A. K., BUCKLEY, R. A. & HUME-ROTHERY, W. (1967). *J. Iron St. Inst.* **205**, 191.

SPARKS, C. J. & BORIE, B. (1966). *Local Atomic Arrangements Studied by X-ray Diffraction.* New York: Gordon & Breach.

STRONG, S. L. & KAPLOW, R. (1967). *Acta Cryst.* **23**, 38.

WARREN, B. E., AVERBACH, B. L. & ROBERTS, B. W. (1951). *J. Appl. Phys.* **22**, 1493.

WARREN, B. E. & MOZZI, R. L. (1966). *Acta Cryst.* **21**, 459.

WOLFF, P. M. DE (1956). *Acta Cryst.* **9**, 682.

Acta Cryst. (1971). A**27**, 109

Dynamical Calculation of Electron Scattering by Plasmons in Aluminum

BY P. A. DOYLE*

School of Physics, University of Melbourne, Parkville, Victoria 3052, *Australia*

(*Received* 16 *July* 1969 *and in revised form* 9 *February* 1970)

Plasmon diffuse scattering (PDS) is calculated for Al(111) systematics using the multi-slice approach to dynamical electron scattering. It is found that PDS contributes strongly to Kikuchi bands, and to the decrease in the mean absorption coefficient which occurs when energy filtering is removed. Thickness fringes are found, which are similar to those for Bragg beams except at low thickness. The different behaviour in this region is explained. The effect of the (111) Kikuchi band on the variation of the path length for plasmon excitation with crystal tilt is considered in detail.

Introduction

The excitation of plasmons in crystals by fast incident electrons has been considered theoretically by several authors. An account of this work has been given by Pines (1964). However, dynamical interactions of the plasmon diffuse scattering (PDS) can be readily implied from experiments with the electron microscope, such as the PDS thickness fringes observed by Kamiya & Uyeda (1961).

These thickness fringes have been predicted by Fujimoto & Kainuma (1962, 1963), Fukuhara (1963), and Howie (1963), who treated the PDS as coherent. Hei-

* Present address: Aeronautical Research Laboratories, Box 4331, G. P. O., Melbourne 3001, Australia.

denreich (1963) treated the PDS as incoherent, attributing the fringes to plasmon excitation in pre- and post-excitation zones. The excitation of a well-defined plasmon cannot be localized except within the crystal boundaries, so that wave amplitudes rather than intensities of the PDS should be summed. Thus PDS is assumed to be coherent throughout the present paper.

Numerical calculations by the above authors have been restricted to the two beam approximation. A method is developed below to include the effects of weak elastic and inelastic beams on first-order PDS, when systematic Bragg beams are excited. This is based on the 'multi-slice' formulation of the wave optical approach to dynamical scattering, as given by Cowley & Moodie (1957). The case of Al(111) systematics will be considered.

Method of calculation

(1) *Bragg beams*

Bragg beams are calculated by using the iterative 'slice' approach of Goodman & Moodie (1965). Absorption is included by allowing the Fourier coefficients, v_h, of the crystal potential $\varphi(x)$ to become complex, so that for the centrosymmetrical crystal,

$$v_h = v_h^r + iv_h^i .$$

Here, v_h^r are the usual coefficients of the thermally smeared out potential, and are based on the atomic scattering factors given by Doyle & Turner (1968). The coefficients v_h^i are related to the absorption coefficients μ_h by

$$v_h^i = \mu_h/2\sigma$$

where $\sigma = \pi e/\lambda E$ for an incident electron of wavelength λ and energy E. The values used for v_h^i include contributions from plasmon, phonon and single electron excitations, and have been calculated for Al(111) systematics, at the required accelerating voltages, as described previously (Doyle 1970, hereafter referred to as I). Table 1 lists the v_h^i for 50 kV electrons.

Table 1. *Calculated values of the absorbing potential* v_h^i *for* (111) *systematic reflexions of* Al *at* 50 kV

(Units: volts

h	v^i (plasmon)	v^i (thermal)	v^i (single electron)	v^i (total)
000	0·485	0·223	0·077	0·785
111		0·198	0·019	0·217
222		0·147	0·017	0·164
333		0·096	0·014	0·110
444		0·055	0·010	0·065
555		0·027	0·007	0·034
666		0·011	0·005	0·016
777		0·002	0·003	0·005
888		−0·001	0·002	0·001

The phase grating amplitudes $F_1(h)$ are given by Fourier transforming the function $\exp[-i\sigma\varphi^P(x)]$, where $\varphi^P(x)$ is the projected crystal potential over a slice of thickness Δz. Goodman (private communication) has shown that the elastic waves $F_N(h)$ at the Nth layer of crystal are then given by

$$F_N(h) = \sum_{h_1} F_{N-1}(h_1)P(h_1)F_1(h-h_1) . \qquad (1)$$

For a crystal tilted at an angle β to the incident beam, the propagation function $P(h)$ is

$$P(h) = \exp\left[+\frac{i\pi\lambda\Delta z}{a^2} - h(h-H')\right]$$

where $H' = 2a\beta/\lambda$, and a is the spacing of the lattice planes.

As stated in I, accurate numerical results for the Bragg beams from Al(111) systematics are obtained if 13 beams and single fundamental unit cell layers are used. These are found to be adequate for plasmon diffuse scattering (PDS) as well, the approach to which will now be considered.

(2) *Plasmon scattered waves*

A method is described by which first order PDS on the systematic line can be calculated, and is then extended to diffuse positions off this line.

Since we will suppose there is no Umklapp process for the plasmon scattering, the additional diffuse wave $\Delta F_N^D(h+p)$ produced in the direction $(h+p)$ in the Nth layer arises only from the Bragg beam in the direction h, and is given by

$$\Delta F_N^D(h+p) = A_{\Delta z}(p)F_{N-1}(h)P(h) . \qquad (2)$$

$A_{\Delta z}(p)$ is the amplitude for plasmon scattering through an angle $\theta = p\lambda/a$, in the layer of thickness Δz, and will be derived later in this section.

The interaction of the PDS at later layers of the crystal is given by

$$F_N^D(h+p) = \sum_{h_1} F_{N-1}^D(h_1+p)P(h_1+p)F_1(h-h_1) . \qquad (3)$$

The calculation proceeds by first storing the amplitudes and phases of the Bragg beams at all layers up to the maximum desired thickness. Then, for each required value of p, PDS is found by carrying out the iteration (3), adding the additional waves at each layer by using (2). In practice, the constant factor $A_{\Delta z}(p)$ is left out until the end of the calculation. It can be shown that the use of (2) and (3) expresses the phases of diffuse waves relative to that of the central Bragg beam. This is also the case for the Bragg beams, so that the additional PDS produced in a given layer has the correct phase relative to that produced in earlier layers.

We can now calculate PDS along the systematic line. However, it is desirable to find the diffuse intensity off this line as well, so that contour maps may be drawn, and the PDS can be integrated over the objective aperture. Examination of Fig. 1 shows that the PDS around the reflexion h, I_h^P, can be written as

$$I_h^P(p',\chi) = A_{\Delta z}^2(p')I_h^D(p'\cos\chi) . \qquad (4)$$

Equation (4) states essentially that the dynamical interactions in this systematics case depend only on the projection of the position in reciprocal space on the systematic line, and that the cross section for plasmon excitation depends only on the angle of scattering from the nearest Bragg beam. The function $I_h^D(p' \cos \chi)$ is derived by using (2) and (3) as described above with $p' \cos \chi = p$, remembering that the factor $A_{\Delta z}(p)$ is omitted. The PDS within the objective aperture around the reflexion h is then given by

$$I_h^P = \int_{\substack{\text{objective} \\ \text{aperture}}} I_h^P(p', \chi) \mathrm{d}\Omega ,$$

which can be rewritten as

$$I_h^P = \frac{2\lambda^2}{a^2} \int_0^{p\max} p' A_{\Delta z}^2(p') \left[\int_0^{\pi} I_h^D(p' \cos \chi) \mathrm{d}\chi \right] \mathrm{d}p' . \quad (5)$$

The value of $p_{\max}$ is related to the diameter of the objective aperture, d, by

$$p_{\max} = ad/2f\lambda$$

where f is the focal length of the objective lens. Equation (5) expresses the PDS as a probability, since the plane wave incident on the crystal is taken as unity.

It now remains to derive an expression for the factor $A_{\Delta z}(p)$. To do this, we will follow an approach suggested by Howie (1963), who pointed out that his treatment of plasmon scattering could be carried through by dividing the range $0 \leq \theta \leq \theta_c$, where θ_c is the cut-off angle for PDS, into a large number of segments of width $\delta\theta$, throughout each of which the cross section can be taken as constant.

The intensities in the various orders of plasmon loss follow a Poisson distribution, whether they are treated kinematically (Blackstock, Ritchie & Birkhoff, 1955) or dynamically (Howie, 1963). Therefore, $A_{\Delta z}(p)$ can be derived by reducing the dynamical calculation described above to a kinematical one. Kinematically, the elastic intensity after thickness Δz is given by

$$I_0^{\text{kin}} = \exp(-\Delta z/\Lambda)$$

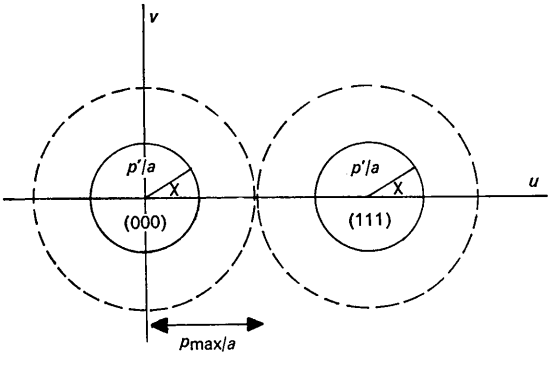

Fig. 1. The definition of p' and χ in the plane of reciprocal space perpendicular to the incident beam, illustrated for two beams only. The dashed line shows the cut-off angle θ_c, which corresponds to $p_{\max} = 0{\cdot}49$ at 50 kV.

where Λ is the path length for plasmon excitation. The phase grating amplitudes are then replaced by

$$F_1(h) = \delta_{h,0} \exp(-\Delta z/2\Lambda) .$$

Again, supposing that momentum is conserved in the inelastic process, the change of wave-vector of the fast electron is equal and opposite to the wave-vector of the plasmon. Therefore, the phase term $P(p)$ in (3) is cancelled by that introduced by the z component of the plasmon wave-vector. This resonance effect is considered more closely in the following section. Then it follows, carrying through the iteration (3) and using (2) for the additional wave in each layer, that the kinematic amplitude for the first plasmon peak in a crystal of thickness $N_3\Delta z$ is given by

$$\psi^{\text{kin}} = N_3 A_{\Delta z}(p) \exp\left(-\frac{N_3 \Delta z}{2\Lambda}\right) .$$

The kinematic single loss intensity produced in the range $\theta \rightarrow \theta + \delta\theta$ is therefore

$$I_{\delta\theta}(1, N_3\Delta z) = N_3^2 A_{\Delta z}^2(\theta) \exp\left(-\frac{N_3 \Delta z}{\Lambda}\right) . 2\pi\theta\delta\theta . \quad (6)$$

Remembering that the Poisson distribution holds for both kinematic and dynamic theory, a second expression for $I_{\delta\theta}(1, N_3\Delta z)$ follows directly from the work of Howie (1963), and can be written as

$$I_{\delta\theta}(1, z) = jc^2(\theta) z^2 (1 - c^2(\theta) z^2)^{J-1} \quad (7)$$

where

$$c^2(\theta) = \left(\frac{m}{2\pi\hbar^2 k}\right)^2 |H_0|^2 . \quad (8)$$

Here, J is the total number of plasmon modes in the crystal, and j is the number in the range $\theta \rightarrow \theta + \delta\theta$. It follows that

$$j = 2\pi k^2 \theta \delta\theta Vc/z,$$

where Vc is the volume of the crystal, and $k = 2\pi/\lambda$.

The matrix element $|H_0|$ has been given by Ferrell (1957) as

$$|H_0|^2 = \frac{2\pi e^2 \Delta E G^{-1}(\theta)}{k^2 Vc} . \quad (9)$$

In (9), ΔE is the plasmon energy, and $G^{-1}(\theta)$ is a function which has been found graphically for Al in I, using a method described by Ferrell (1957). Finally, from conservation of energy and momentum,

$$\frac{m}{(\hbar k)^2} = \frac{1}{2E(\theta^2 + \theta_E^2)} \text{ where } \theta_E = \Delta E/2E . \quad (10)$$

Inserting (8) (9) and (10) in (7), and taking the limit of large J,

$$I_{\delta\theta}(1, N_3\Delta z) = \frac{N_3 \Delta z \theta_c \theta \delta\theta G^{-1}(\theta)}{a_0(\theta^2 + \theta_E^2)} \exp\left(-\frac{N_3 \Delta z}{\Lambda}\right) . \quad (11)$$

Equating (6) and (11), $A_{\Delta z}(\theta)$ is found to be

$$A_{\Delta z}^2(\theta) = \frac{\theta_E G^{-1}(\theta)}{2\pi a_0(\theta^2 + \theta_E^2)} \cdot \frac{\Delta z}{N_3} . \quad (12)$$

When this expression is used in the dynamical calculation, the total first loss intensity is proportional to z for low values of z, as is required to agree with the Poisson distribution law, and hence to conserve the total intensity.

Accuracy of the calculation

Contributions to PDS arise from several of the normal modes for plasmons. Howie (1963) argued that no serious error is introduced by considering the excitation of only the mode for which the energy momentum relations are exactly satisfied. This approximation is incorporated in equation (12).

By including a phase term $\exp(ik_{jz}z_N)$ on the PDS produced at a depth z_N in the crystal in the dynamical calculations, the contribution from a mode other than that with $k_{jz}=0$ can be obtained. For small objective aperture sizes (corresponding to $p_{\max}>0{\cdot}25$), it is found that including contributions from several plasmon modes with small k_{jz} alters the relative diffuse intensities around inner reflexions by only 1 to 2%. This increases to about 8% when the whole of the PDS is included ($p_{\max}\simeq 0{\cdot}5$).

Ferrell (1957) gave an expression for θ_c, which can be written for Al as

$$\theta_c=0{\cdot}74(E_0/E)^{1/2}$$

where E_0 is the Fermi energy. To test the self-consistency of the calculation, absorption due to processes other than plasmon scattering is omitted, and the PDS is integrated out to θ_c around each Bragg beam.* The total PDS is found to be up to 10% lower than predicted by the Poisson distribution, being least accurate for crystal thicknesses near the path length. This error may be due to the 'resonance effect' discussed above.

Profile of plasmon diffuse scattering

The profile of the first order PDS, $I_h^P(p',\chi)$, calculated for N-beam systematics, around the two strong beams when the (111) reflexion of Al is satisfied, is shown in Fig. 2(*a*). This is for a thickness of 910 Å and for 50 kV electrons. The characteristic decrease of intensity between the two strong beams, or equivalently, the (111) Kikuchi band, is clearly visible. Howie (1963) showed that this experimentally observed phenomenon is caused by anomalous absorption, which in turn results from phonon and single electron excitations (Table 1).

The asymmetry is shown clearly by scanning the PDS along a line in reciprocal space, such as the dashed line in Fig. 2(*a*). This scan is shown in Fig. 2(*b*). Since the effect relies on the different absorption occurring for different Bloch waves excited in the crystal, it should become more apparent with increasing thickness. By integrating the PDS inside the positions of the (111) Kikuchi lines, and comparing this with the integrated PDS near the two strong beams but outside

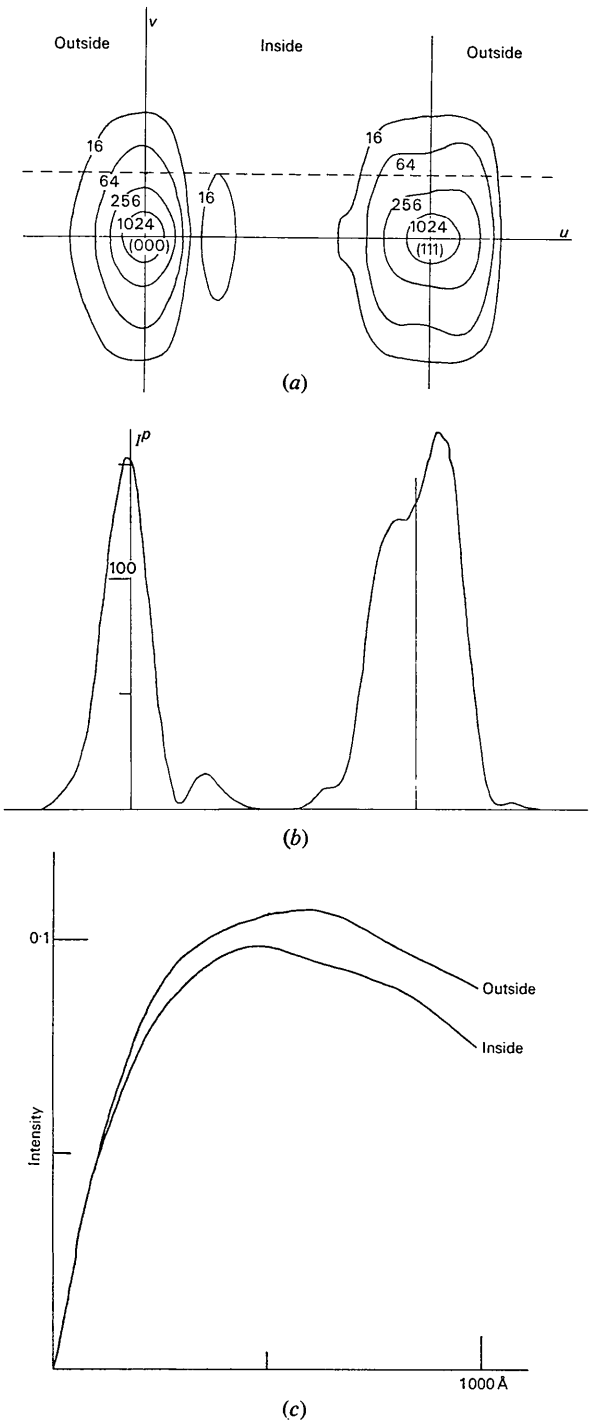

Fig. 2. The contour map for first order PDS, given by equation (4), around the two strong beams when the (111) reflexion is satisfied, is shown in (*a*). This is for 50 kV, and 910 Å of Al(111) systematics. $I_h{}^P(p',\chi)$ along the dashed line in (*a*) is shown in (*b*). The total first order PDS near the two strong beams 'inside' and 'outside' the (111) Kikuchi lines as illustrated in (*a*) is shown as a function of thickness in (*c*).

* Numerical integration is carried out to a consistency of 1% throughout the present paper. The value of $p_{\max}$ corresponding to θ_c at 50 kV is 0·49.

these lines, as illustrated in Fig. 2(*a*), the increase with thickness of the asymmetry in the distribution can be found, as shown in Fig. 2(*c*). The maximum first order PDS intensity occurs well below the theoretical path length (841 Å) for plasmon excitation at this voltage, since absorption due to other inelastic processes is included for both Bragg beams and PDS.

Since thickness fringes are still dominant at 1000 Å of Al, the profile of the PDS is strongly dependent on thickness. Fig. 3 shows the contour map for the same case as Fig. 2(*a*), except that the thickness has been increased from 910 to 1000 Å. The omission of the resonance effects mentioned in the previous section will preferentially decrease the PDS outside the (111) Kikuchi band for this two-beam tilt, because of the curvature of the Ewald sphere. This may be partly responsible for the rapid fall-off of the contours in these regions. Thus the asymmetry may be slightly greater than predicted here, though the effect on the integrated intensity of Fig. 2(*c*) is expected to be small.

Thickness fringes for plasmon scattering

The variation with thickness of the first order PDS integrated over the objective aperture is shown for the (000) and (111) beams in Fig. 4(*a*) and (*b*) respectively, and is compared with that for the corresponding Bragg beams. These graphs are for Al(111) systematics with the (111) reflexion satisfied, and for 40 kV electrons. The value of p_{max} used was 0·18, which corresponds to the objective aperture size used in the determination of absorption coefficients by Watanabe (1964).

(*a*) *Qualitative interpretation*

In general, the profiles of the thickness fringes are similar to those for the Bragg beams, except at low thickness. In the bright field [Fig. 4(*a*)], the first peak of the elastic intensity occurs at the edge of the crystal, whereas that for the PDS is shifted to a finite thickness. This is expected, since the excitation of plasmon losses with the electron in an 'advance excitation zone' as proposed by Heidenreich (1963) is not included in the present treatment. This shift causes the first fringe in the bright field PDS to have half the usual periodicity and was also predicted by Fukuhara (1963). However, Watanabe (1964) has pointed out that the intensity of this fringe is experimentally far greater than was predicted by Fukuhara, and this is in qualitative agreement with the present calculations.

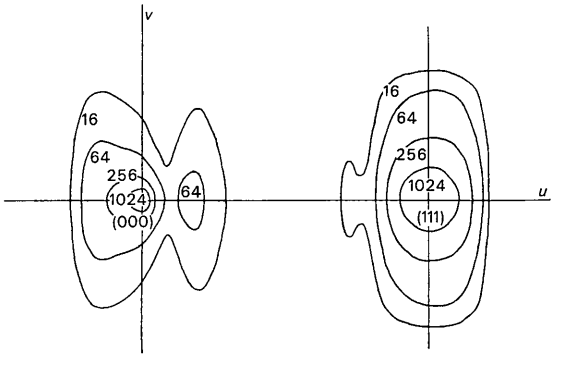

Fig. 3. As for Fig. 2(*a*), except that the crystal thickness is 1000 Å.

The higher order thickness fringes in the bright field have peak values shifted towards greater thickness relative to those for the elastic beam, by an amount which decreases with increasing fringe number. This is because PDS in bright field is generated from the central Bragg beam only, which can therefore contribute most strongly near its maxima. A similar argument explains the shift of the peaks in the PDS fringes in the dark field as well [Figure 4(*b*)]. For low thickness the PDS in dark field increases proportionally to z^3. This is because PDS in this region at low thickness results principally from a permutation of an elastic scattering, which is proportional to z^2 for low z, and an inelastic scattering, which is proportional to z. This argument is valid for all beams with $h \neq 0$. This z^3 appearance rapidly disappears, however, once significant intensity has been scattered to the elastic (111) reflexion. Note that the total PDS in the whole diffraction pattern increases proportionally to z for low z, as mentioned previously, since the bright field is initially dominant.

(*b*) *Measurement of the mean absorption coefficient*

Watanabe (1964) has measured the mean absorption coefficient for Al at 40 kV. He denoted the values found with and without energy filtering by μ_0 and $[\mu_0]$ respectively. It was found in I that the value of μ_0 calculated from simple physical models for the inelastic scattering processes involved agreed with the experimental value within 25 %. The bright field experiment was considered more suitable, since the dark field value would be increased by spherical aberration. The agreement for $[\mu_0]$ is considered in this section.

From the N-beam systematic calculations of thermal diffuse scattering by Doyle (1969), it appears that this form of diffuse scattering will contribute very weakly to thickness fringes. If we also suppose that scattering by single electron excitations does not contribute significantly to thickness fringes, then the lower values measured for $[\mu_0]$ compared with those for μ_0 should be explicable in terms of PDS.

Table 2. *Comparison of theory and experiment for the mean absorption coefficient at* 40 kV

Theoretical value = $2{\cdot}35 \times 10^{-3}$ Å^{-1}
Units: $\times 10^{-3}$ Å^{-1}.

		Calculated*	Experiment
Dark field	μ_0	2·21	3·24, 3·20
	$[\mu_0]$	1·59, (1·67)	2·58, 2·2
Bright field	μ_0	2·20	2·98, 3·02
	$[\mu_0]$	1·50, (1·80)	1·82, 1·78, 1·54

* The first calculated value shown for $[\mu_0]$ was found from the first two maxima in the thickness fringes. The value in brackets was found from the second and third maxima.

Since Watanabe (1964) used a two-beam theory in interpreting the thickness fringes, this approximation must be used to find values of $[\mu_0]$ from the fringes of Fig. 4(*a*) and (*b*), which represent the elastic plus the first plasmon loss intensity. The standard method used, as described in I, yields a value for each pair of maxima in the fringes. Table 2 shows values of $[\mu_0]$ calculated in this way, together with those for μ_0, which have been taken from I.

The theoretical values found from the first and second peaks in the fringes are lower than those found from the second and third peaks, for both bright and dark fields. This is expected, since the relative intensity of higher order plasmon losses, which will also contribute to the thickness fringes, increases with increasing thickness. Therefore, considering the theoretical values of $[\mu_0]$ measured from low thickness, the percentage decrease relative to the μ_0 values is seen to be comparable with the experimental decrease. The agreement is not exact, since some multiple PDS is present, and it was assumed above that no other inelastic process contributes significantly to the fringes. Again, the experiment is subject to errors, such as chromatic aberration, which have been ignored.

Plasmon path length*

Ishida, Mannami & Tanaka (1967) measured the path length, Λ, for plasmon excitation for Al in the (111) orientation. They found crystal thicknesses by fitting two-beam rocking curves to the bright field rocking curve. This gives thicknesses 7 to 8% too high, as is approximately the case if thickness fringes are used, and this appears as a systematic error in their determination of Λ. Correcting their measured value of Λ for this effect, the experimental value at 50 kV becomes 930 Å, in reasonably good agreement with the theoretical value of 841 Å.

Ishida, Mannami & Tanaka (1967) and also Tonomura & Watanabe (1967), found that Λ for the bright field from Al was greater for negative than for positive values of the two-beam deviation parameter, x. The former authors interpreted this as being due to an anomalous absorption coefficient for PDS, $\Delta\mu$, using two-beam theory. Using the relation

$$\Delta\mu \simeq -\Delta\Lambda/\Lambda^2$$

where $\Delta\Lambda$ is the anomaly in the path length, their experimental value was equivalent to $\Delta\mu = -0{\cdot}1 \times 10^{-3}$ Å^{-1}. The minus sign implies that the Bloch wave on the second branch of the two-beam dispersion surface is preferentially transmitted. Ohtsuki (1968) pointed out that the plasmon will polarize the lattice, causing a decrease in the thermal and single electron contributions to the absorption coefficients. Thus when Λ is determined by taking for example the ratio of the elastic to the first plasmon loss intensities, $I_0(x)$ and $I_1(x)$ respectively, the asymmetry appears, since the plasmon–phonon and, to a lesser extent, the plasmon–single electron coupling cause a lower value of μ_h to operate on $I_1(x)$.

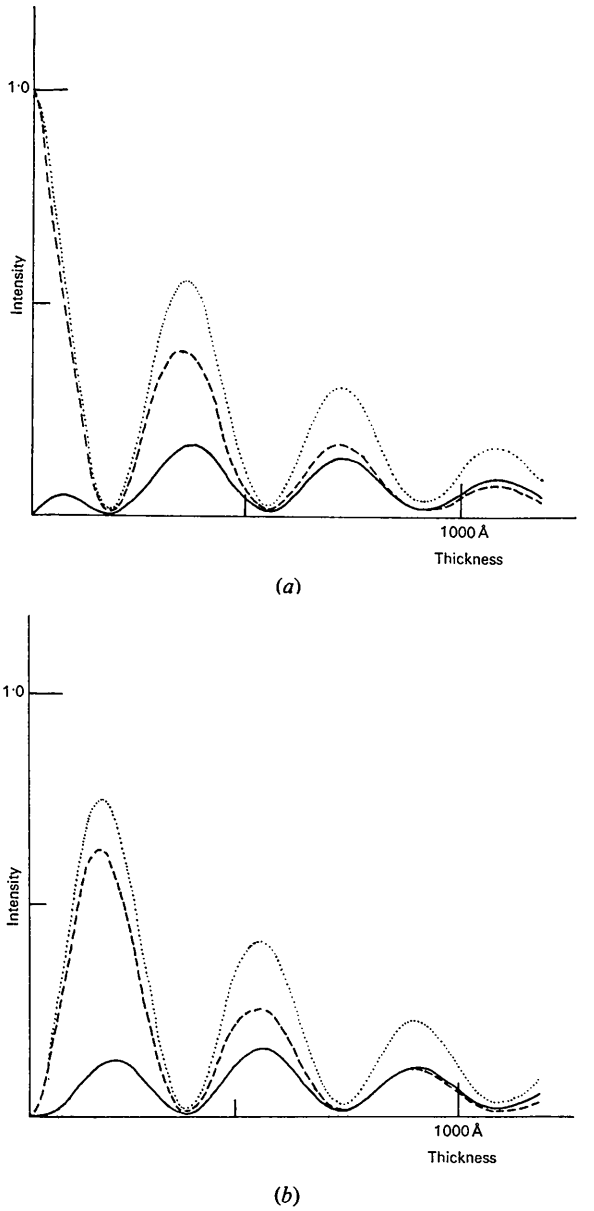

Fig. 4. The first order PDS integrated over the objective aperture is shown as a function of thickness by the full lines in (*a*) and (*b*), which are for the central and (111) beams respectively. These are for 40 kV and an aperture size corresponding to $p_{max} = 0{\cdot}18$, for the (111) reflexion satisfied. The dashed lines are the corresponding thickness fringes for the Bragg beams. The sums of these two intensities are denoted by dotted lines. All intensities are expressed as probabilities.

* *Note added in proof:* J. C. H. Spence (private communication) pointed out that the sign convention for $\Delta\mu$ used here, and also implicitly used by Ishida, Mannami Tanaka, should be reversed. The present conclusions concerning the Kikuchi band remain valid, though the effect discussed by Ohtsuki would oppose rather than enhance the observed asymmetry.

However, as emphasized by Tonomura & Watanabe (1967), the (111) Kikuchi band passes across the objective aperture as the crystal is tilted. This effect is included in the present calculations. Fig. 5 shows the ratio I_0/I_1 calculated as a function of x for the bright field, for several crystal thicknesses. The accelerating voltage is 50 kV, and p_{max} was taken as 0·49 to include the whole of the first plasmon loss around the central beam. Following Ishida, Mannami & Tanaka, an estimate of the value of $\Delta\mu$ implied by the asymmetry in the graphs of Fig. 5 can be found by treating them as two-beam rocking curves. Then, the bright field rocking curve is given by

$$I_0(x) = \frac{\exp(-\mu_0 z)}{2(1+x^2)}\left[(1+2x^2)\cosh\left(\frac{\Delta\mu z}{\sqrt{1+x^2}}\right) + \cos\left(\frac{2\pi z\sqrt{1+x^2}}{\xi g}\right) + 2x\sqrt{1+x^2}\sinh\left[\left(\frac{\Delta\mu z}{\sqrt{1+x^2}}\right)\right]\right] = S + A \qquad (13)$$

where S and A are the terms in (13) symmetrical and antisymmetrical with respect to x.

It is convenient to define a function $C(\Delta\mu)$ given by

$$C(\Delta\mu) = \int_0^{x_{max}} A\,dx \Big/ \int_{-x_{max}}^{x_{max}} I_0(x)\,dx\,. \qquad (14)$$

The value taken for x_{max} is 2·58, which corresponds to satisfying the (222) reflexion at 50 kV. Values of C can be found from the graphs of Fig. 5, since the appropriate normalization [corresponding to the bottom line of (14)], is readily obtainable. Thus by calculating $C(\Delta\mu)$ numerically using (14), $\Delta\mu$ can be found for each thickness, and these are listed in Table 3.

Table 3. *Values of $\Delta\mu$ due to the path length anomaly**

Thickness (Å)	$\mu(\times 10^{-3}$ Å$^{-1})$
250	0·22
500	0·38
750	0·26
1,000	0·44

* The large spread of values raises the question of the validity of interpreting the anomaly as due to a value for $\Delta\mu$. Unfortunately, the length of the calculation of rocking curves for diffuse scattering prevents a detailed study of the variation of $\Delta\mu$ with thickness.

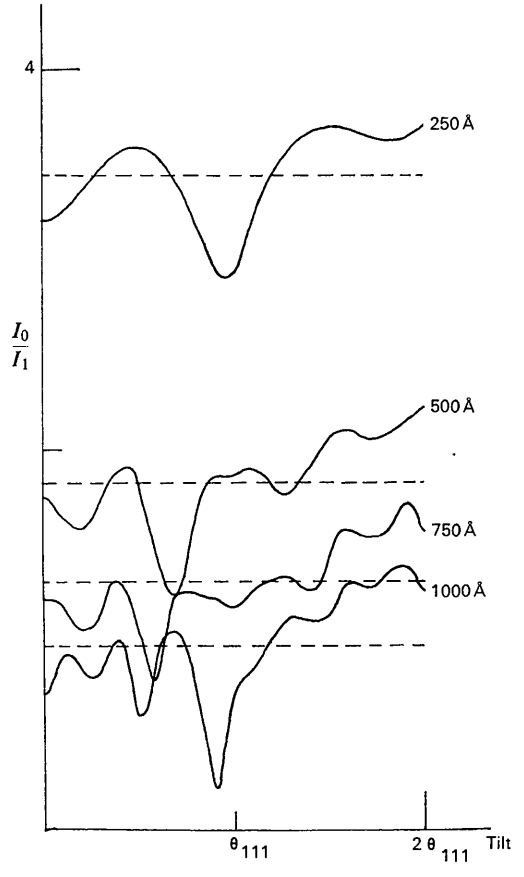

Fig. 5. The ratio I_0/I_1 plotted against crystal tilt for several thicknesses at 50 kV. The dashed lines are the average values.

The values of $\Delta\mu$ in Table 3 are positive. This is because $I_1(x)$ involves an integration over the aperture, or equivalently, over a range of tilts with suitable weighting factors. Thus $I_1(x)$ cannot completely follow fluctuations in the Bragg beam with tilt. For example, when both $I_0(x)$ and $I_1(x)$ are low near $x=0$ for 250 Å (Fig. 6), I_0/I_1 in Fig. 5 is also low. The gross effect in $I_0(x)$ is the asymmetry about $x=0$. Since $I_1(x)$ is unable to follow this completely, I_0/I_1 is in general greater for positive than for negative values of x, so that $\Delta\mu$ is positive. Since the rocking curve asymmetry increases with thickness, $\Delta\mu$ is also expected to increase. This can be seen in Table 3, though there is a wide spread of values.

Ishida, Mannami & Tanaka measured an asymmetry opposite to that in Fig. 5, which became less apparent with increasing thickness, as would be expected from the preceding argument. The asymmetry implies, barring systematic experimental errors, that there is an additional effect such as that suggested by Ohtsuki (1968), which not only introduces asymmetry in $A(x)$, but is strong enough to reverse it. Taking the average value of $\Delta\mu$ from Table 3, such an effect corresponds to $\Delta\mu = (-0{\cdot}3 - 0{\cdot}1)\times 10^{-3} = -0{\cdot}4\times 10^{-3}$ Å^{-1}, *i.e.* it is about four times stronger than measured by the above authors. The contribution to $\Delta\mu$ from plasmon–phonon coupling estimated by Ohtsuki (1968) was $-0{\cdot}044\times 10^{-3}$ Å^{-1}. Further theoretical investigation of this effect may therefore prove fruitful. It may, for example, be partially responsible for the disappearance of thermal streak patterns from the 16 eV loss pattern from Ge, as observed by Watanabe (1964).

As we have seen, the difficulty in measuring $\Delta\mu$ is caused by partially averaging over tilt for $I_1(x)$, but not for $I_0(x)$. Unless lengthy calculations of the type de-

scribed here are performed, meaningful values of $\Delta\mu$ may not be obtainable by the experimental methods used by the authors listed above. Indeed, an accurate correction for the influence of the Kikuchi band may require as well further consideration of the resonance effects discussed in an earlier section, since these are dependent on crystal tilt.

Conclusions

The principal conclusions drawn above are listed below.

(1) The total first plasmon loss intensity for low thickness is proportional to z, in agreement with the Poisson distribution. This is also true for PDS around the central beam, but the first order loss near other beams is initially proportional to z^3.

(2) The PDS forms Kikuchi bands, in particular the (111) band from Al, which appears when the (111) reflexion is satisfied as a characteristic decrease of diffuse intensity between the two strong beams. This effect becomes more marked with increasing thickness, and is caused by the Bormann effect acting on the diffuse scattering.

(3) Plasmon scattering forms thickness fringes which, except at low thickness, closely resemble those for Bragg beams. The different behaviour at low thickness can be understood qualitatively, and is in agreement with experiment.

(4) PDS offers a reasonable account of the decrease in the measured value of the mean absorption coefficient, as determined for example by Watanabe (1964), when energy filtering is removed.

(5) The theoretical path length of 841 Å calculated here for plasmon excitation by 50 kV electrons in Al is in reasonably good agreement with that measured by Ishida, Mannami & Tanaka (1967), which, when corrected for the effect of weak systematic beams, is 930 Å.

(6) The passage of the (111) Kikuchi band across the objective aperture as the crystal is tilted tends to mask rather than cause the plasmon path length anomaly observed by Tonomura & Watanabe (1967) and by Ishida, Mannami & Tanaka (1967). The present calculation, though ignoring the resonance effects discussed which could have a significant bearing in this case, suggests that the anomaly is about four times greater than found by the above authors. This exceeds by almost an order of magnitude the plasmon–phonon contribution as estimated by Ohtsuki (1968).

The author is indebted to Dr P. S. Turner for permission to build on his computer program dealing with Bragg beam calculation, and to Professor J. M. Cowley and C. J. Ryan for several helpful discussions. This work was partially supported by a grant from the Australian Research Grants Committee.

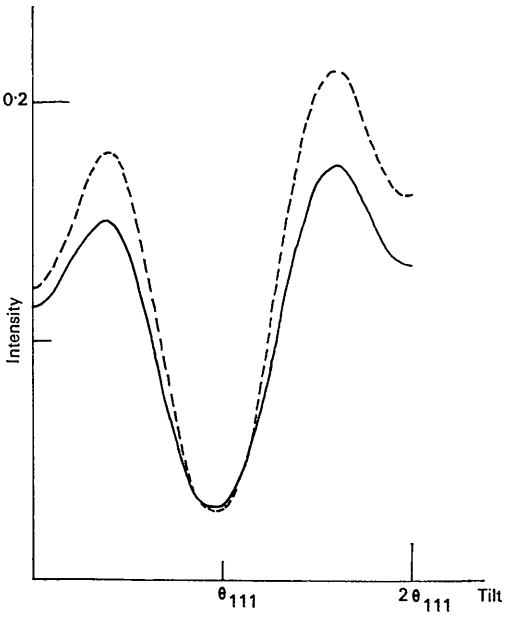

Fig. 6. First order PDS (full line) and Bragg beam (dashed line) rocking curves for bright field at 250 Å thickness and 50 kV. The intensities are expressed as probabilities, though the Bragg beam curve has been decreased by a factor of three to allow a ready comparison.

References

BLACKSTOCK, A. W., RITCHIE, R. H. & BIRKHOFF, R. D. (1955). *Phys. Rev.* **100**, 1078.
COWLEY, J. M. & MOODIE, A. F. (1957). *Acta Cryst.* **10**, 609.
DOYLE, P. A. (1969). *Acta Cryst.* A**25**, 569.
DOYLE, P. A. (1970). *Acta Cryst.* A **26**, 133.
DOYLE, P. A. & TURNER, P. S. (1968). *Acta Cryst.* A**24**, 390.
FERRELL, R. A. (1957). *Phys. Rev.* **107**, 450.
FUJIMOTO, F. & KAINUMA, Y. (1962). *J. Phys. Soc. Japan*, 17B-II, 140.
FUJIMOTO, F. & KAINUMA, Y. (1963). *J. Phys. Soc. Japan*, **18**, 1792.
FUKUHARA, A. (1963). *J. Phys. Soc. Japan*, **18**, 496.
GOODMAN, P. & MOODIE, A. F. (1965). *Intern. Conf. Electron Diffraction and Crystal Defects.* Melbourne. ID-1, ID-2.
HEIDENREICH, R. D. (1963). *J. Appl. Phys.* **34**, 964.
HOWIE, A. (1963). *Proc. Roy. Soc.* A**271**, 268.
ISHIDA, K., MANNAMI, M. & TANAKA, K. (1967). *J. Phys. Soc. Japan*, **23**, 1362.
KAMIYA, Y. & UYEDA, R. (1961). *J. Phys. Soc. Japan*, **16**, 1361.
OHTSUKI, Y. H. (1968). *Phys. Letters*, 27A, 65.
PINES, D. (1964). *Elementary Excitations in Solids.* New York: Benjamin.
TONOMURA, A. & WATANABE, H. (1967). *Jap. J. Appl. Phys.* **6**, 1163.
WATANABE, H. (1964). *Jap. J. Appl. Phys.* **3**, 480.